ACS APPLIED MATERIALS & INTERFACES

Research Article

www.acsami.org

Composite Transparent Electrode of Graphene Nanowalls and Silver Nanowires on Micropyramidal Si for High-Efficiency Schottky Junction Solar Cells

Tianpeng Jiao,[†,‡,#] Jian Liu,[†,§,#] Dapeng Wei,[*,†] Yanhui Feng,[‡] Xuefen Song,[†] Haofei Shi,[†] Shuming Jia,[†] Wentao Sun,[*,§] and Chunlei Du[†]

[†]Chongqing Key Laboratory of Multi-scale Manufacturing Technology, Chongqing Institute of Green and Intelligent Technology, Chinese Academy of Sciences, Chongqing 400714, PR China

[‡]School of Mechanical Engineering, University of Science and Technology Beijing, Beijing 100083, PR China

[§]Key Laboratory for the Physics and Chemistry of Nanodevices& Department of Electronics, Peking University, Beijing 100871, PR China

Supporting Information

ABSTRACT: The conventional graphene-silicon Schottky junction solar cell inevitably involves the graphene growth and transfer process, which results in complicated technology, loss of quality of the graphene, extra cost, and environmental unfriendliness. Moreover, the conventional transfer method is not well suited to conformationally coat graphene on a three-dimensional (3D) silicon surface. Thus, worse interfacial conditions are inevitable. In this work, we directly grow graphene nanowalls (GNWs) onto the micropyramidal silicon (MP) by the plasma-enhanced chemical vapor deposition method. By controlling growth time, the cell exhibits optimal pristine photovoltaic performance of 3.8%. Furthermore, we improve the conductivity of the GNW electrode by introducing the silver nanowire (AgNW) network, which could achieve lower sheet resistance. An efficiency of 6.6% has been obtained for the AgNWs-GNWs-MP solar cell without any chemical doping. Meanwhile, the cell exhibits excellent stability exposed to air. Our studies show a promising way to develop simple-technology, low-cost, high-efficiency, and stable Schottky junction solar cells.

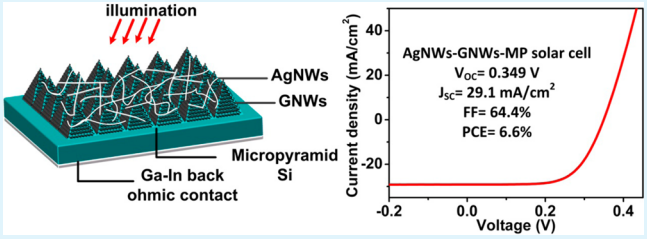

KEYWORDS: *one-step growth, graphene nanowalls, three-dimensional Si, solar cells, silver nanowires, composite electrode, high efficiency, stability*

1. INTRODUCTION

The aggravating energy crisis has promoted considerable efforts to explore solar cells. To date, crystalline silicon (Si) has occupied the majority of the photovoltaic materials market due to the advantages of natural abundance, good properties, and mature processing technique.[1,2] However, for the traditional Si solar cells based on the P−N junction, the high cost from complicated processing and excessive consumption of Si hinders popularization and progress.[3,4]

Graphene, a single atomic layer of carbon hexagons, has attracted great attention because of its superior properties, including tunable work function, high electrical conductivity, high optical transmittance, and low sheet resistance.[5−7] Graphene film could be grown via a chemical vapor deposition (CVD) process, and is transferred onto Si to form the Schottky junction, which could separate light-generated carriers. The first graphene-Si (Gr-Si) solar cell was fabricated by Li et al. in 2010, which achieved an efficiency of 1.5%.[8] Lately, a lot of effort has been made to improve the efficiency of the Gr−Si solar cell. In various Si-based solar cells, Si micropyramid (MP), Si nanowire, Si nanocone, and Si nanohole array, which serve as light-trapping structures, are effective means to increase the light absorption for solar cells.[9−12] Xie et al. fabricated the graphene-Si nanowire solar cell with efficiency of 2.15%.[13] Feng et al. adopted Si pillar-array structures to replace planar Si in Gr−Si solar cells and got a pristine efficiency of about 2.9%, and the PCE could be further improved to 4.35% by HNO_3 doping.[14] Zhang et al. reported a few-layer graphene−Si microhole solar cell with pristine efficiency of 3.468%, with efficiency increasing to 10.297% after HNO_3 doping.[15] Chemical doping of graphene is considered an efficient way to inject a majority of carriers, reduce sheet resistance, and heighten the work function of graphene, which could effectively improve the performance of the Gr−Si solar cells.[16,17] Recently, an efficiency of 14.5% was achieved by introducing TiO_2 as an antireflection coating and by HNO_3 doping.[18] However, the chemically doped Gr−Si solar cells degrade seriously over time because of the subdued doping effect. Meanwhile, after eliminating the chemical doping, the

Received: June 23, 2015
Accepted: August 26, 2015
Published: August 26, 2015

DOI: 10.1021/acsami.5b05565
ACS Appl. Mater. Interfaces 2015, 7, 20179−20183

pristine efficiency of the Gr−Si solar cells is still low, not exceeding 4%.[18−20] On the other hand, for the previously reported Gr−Si solar cells, transferring CVD graphene onto Si wafer was inevitable. The graphene transfer process has limited the practical application in solar cells because of the fussy technology, increased cost, and inevitable loss of quality of graphene through the traditional polymer-mediated transfer method.[21−23] More importantly, the transfer method is not well suited for conformal coating of graphene on three-dimensional (3D) structural surfaces, such as Si nanocone, nanocolumn, nanohole array, and so on.

Graphene nanowalls (GNWs), consisting of cross and vertical graphene sheets, could be directly produced on Si or other substrates by the plasma-enhanced chemical vapor deposition (PECVD) method.[24,25] Here, we directly grow a GNW network on the micropyramidal Si wafer while avoiding the graphene transfer process, and fabricate graphene nanowall−micropyramidal Si Schottky junction (GNWs-MP) solar cells with obvious pristine photovoltaic performance. The micropyramidal morphology can effectively suppress the light reflectance, causing the increase of J_{SC}. We also investigate the influence on the cell with different growth times.To further improve the conductivity of the GNWs, the silver nanowire (AgNWs) network is fabricated onto the GNWs by a simple brush-painting process. Ultimately, the AgNWs-GNWs-MP solar cell gets to an efficiency of 6.6%. Moreover, the cell shows better stability than the Gr−Si and carbon nanotube-Si (CNT-Si) solar cells with chemical doping.

2. EXPERIMENTAL SECTION

2.1. MP Preparation. An N-type ⟨100⟩ single-crystalline Si (resistivity of 1−3 Ω cm^{-1}) with 300 nm SiO_2 is used as the substrate. An open window of 2.5 × 2.5 mm^2 was exposed to HF for 3 min to remove the SiO_2 layer, and was defined as the effective work area of the solar cells. The MP textures were fabricated by an anisotropic etching method in KOH (3 wt %)/$NaSiO_3$ (1 wt %)/isopropyl alcohol (8 vol%) at 85 °C for 30−40 min. Then the wafers were treated by standard RCA (Radio Corporation of America) cleaning, followed by 1% HF treatment for 1 min, before GNWs growth.

2.2. GNWs Preparation. First, the target substrate was heated to 750 °C under the atmosphere of hydrogen (H_2). Then the substrate should be rinsed with H_2 plasma for 10 min to clean the wafer. The radiofrequency (RF) power and the H_2 flow rate were 100 W and 10 standard cubic centimeters per minute (SCCM), respectively. Gas mixture of methane (CH_4):H_2 = 6:6 SCCM was used with RF power of 50 W, and the growth pressure is around 40 Pa. The growth time ranged from 30 to 45 min. Finally, the samples were quickly cooled to room temperature with H_2 as protective gas.

2.3. Solar Cell Fabrication. Eutectic Ga−In that could form back contact with Si was used as back electrode. AgNWs with average diameters of 30 nm in alcohol (10 mg/mL) were purchased from Blue Nano. The AgNWs were continuously brushed onto GNWs using a general paint brush at room temperature and then dried on a hot plate at 80 °C for 5 min to remove the solvent.

2.4. Characterization. The quality of GNWs was characterized by Raman spectroscopy (inVia Reflex) with 532 nm laser, and the sheet resistance (R_{SH}) was measured by four-point probe system. The transmittance and reflectance of the samples were measured by UV−visible spectrophotometer (Lambda35) with an integrating sphere. The morphologies of the GNWs were characterized by high-resolution scanning electron microscope (SEM; JSM-7800F). The performances of the solar cells were measured by using a Keithley 2400 source meter and a solar simulator under AM1.5 illumination.

3. RESULTS AND DISCUSSION

For the planar Si, over 35% light is lost on the surface because of the high reflectance. Micropyramidal Si structure could effectively trap incident light with a simple and inexpensive anisotropic etching process.The morphologies of the MP are shown in Figure S1 (Supporting Information) with different etching times of 30, 35, and 40 min. The 30 min etching produces abundant pyramids, but the sizes are small. For the 35 min etching, the major pyramids get more uniform shapes with a large size of about 8−10 μm. After 40 min etching, massive pyramids appear. Reflectance measurement results are presented in Figure S2 (Supporting Information). The lowest reflectance of the MP, which was obtained with 35 min etching, could be as low as ∼10% in the range of 500−1000 nm. Therefore, we adopt the MP of 35 min etching as the substrate in our solar cells.

For the GNWs−MP solar cells, the growth time of the GNWs is crucial to the performance of the cells. In this work, four groups of experiments with growth times of 30, 35, 40, and 45 min are performed. The morphologies of the GNWs, grown on the MP substrate with different growth times, are observed by SEM in Figure 1b−e. At 30 min, the small-sized graphene sheets

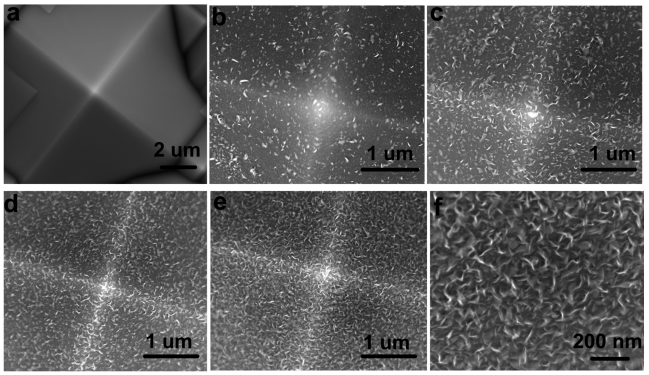

Figure 1. (a−e) Top-view SEM images of micropyramid Si (MP) and the graphene nanowalls directly grown on the MP with growth time of 30, 35, 40, and 45 min, respectively. (f) SEM image of the GNWs with 45 min growth time with higher magnification.

sporadically distribute on the surface of MP. As the growth time increases, the grain sizes of graphene sheets become enlarged, and the uniformity is better. The continuous leaf-like graphene sheets have absolutely covered the wafer of MP at 45 min, and form a compact 3D conducting GNW network, as shown in Figure 1e and f.

Raman analysis is an efficient way to characterize the quality of the GNWs. As shown in Figure 2a, the D peak (∼1350 cm^{-1}), G peak (∼1585 cm^{-1}), and 2D peak (∼2695 cm^{-1}) could be observed in all the samples. Meanwhile, the shoulder peak (G′ peak) and sharp D peak are also visible, which are connected with the defects and edges from small-size graphene sheets. The full width at half-maximum, I_{2D}/I_G and I_D/I_G are the important parameters to estimate the layers and defects of graphene. The value of I_{2D}/I_G ranges from 0.49 to 0.97, and the full width at half-maximum values are ∼55 to ∼70 cm^{-1}, indicating graphene sheets with few layers. The I_D/I_G decreases from 1.75 to 1.0, with the increase of growth time from 30 to 45 min (Figure 2b), which demonstrates that GNWs have lower defect density and larger grain size with longer growth time. Figure 2c shows the optical transmittance spectra of the GNWs with different growth times. Obviously, the transmittance of GNWs decreases as the growth

DOI: 10.1021/acsami.5b05565
ACS Appl. Mater. Interfaces 2015, 7, 20179−20183

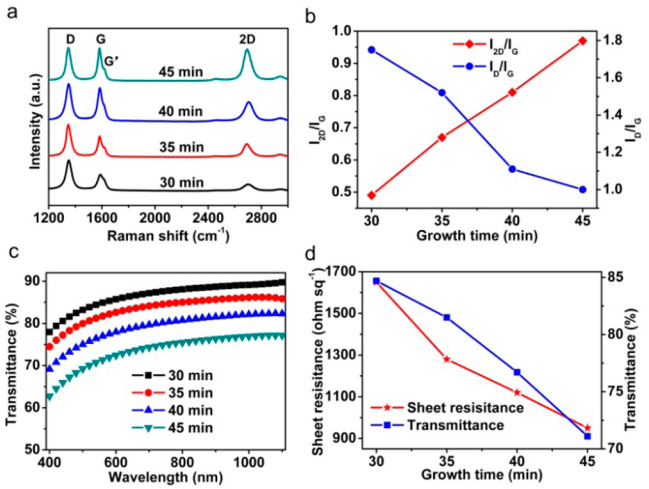

Figure 2. (a,b) Raman spectrum and the intensity ratios I_{2D}/I_G and I_D/I_G of the GNWs corresponding to growth times of 30, 35, 40, and 45 min. (c) Transmittance of GNWs in the range 400−1100 nm. (d) Sheet resistance and transmittance at 550 nm of the GNWs with different growth times.

time increases. The values of the transmittance at 550 nm (T_{550}) and average sheet resistance (R_{SH}) at different growth times are exhibited in Figure 2d. The T_{550} of 30 min GNWs is 84.7%, while the relevant R_{SH} is about 1650 Ω/sq. At 45 min, although the T_{550} reduces to 71.1%, the R_{SH} could also decrease to about 950 Ω/sq. It is clear that the improvement of the R_{SH} is accompanied by the decline of the transmittance.

Figure 3a illustrates the schematic of the GNWs-MP solar cells. The conformal coverage of GNWs could form a Schottky

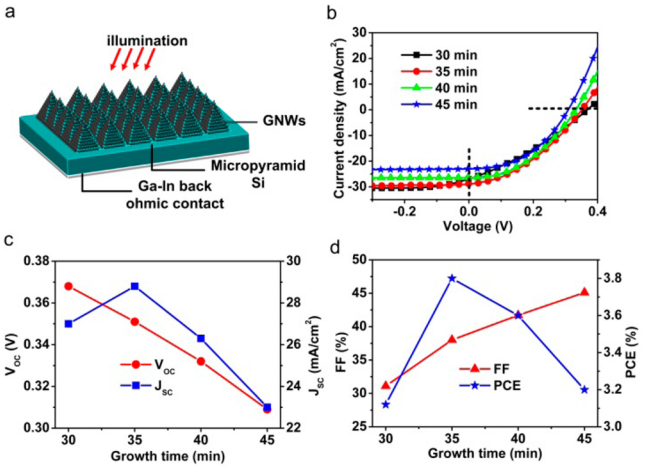

Figure 3. (a) Illustration of the GNWs-MP solar cell structure. (b) Current density−voltage (J−V) curves with different growth times under AM1.5 illumination. (c,d) Plots of V_{OC}, J_{SC}, FF, and PCE as functions of growth time.

junction with MP Si, and generates built-in potential across the Si side. Under illumination, the micropyramidal Si could effectively absorb the incident light and produce electron−hole pairs. Then photogenerated electron−hole pairs would be separated by built-in electric field. The holes are pulled to the GNW side, and a Ga−In cathode could collect the electrons.

Figure 3b shows the light current density−voltage (J−V) curves of the GNWs-MP solar cells with growth time of 30−45 min. As the growth time increases from 30 to 45 min, the fill factor (FF) is improved from 31.0% to 45.1%, which benefits from the reduction of R_{SH}. The open circuit voltage (V_{OC}) is gradually decreased from 0.368 to 0.309 V (Figure 3c), meaning that the longer growth time could result in the decrease of the work function of the GNWs. For the J_{SC}, the largest value of 28.7 mA/cm^2 appears at the point of 35 min, because the longer growth time would suffer from low transmittance, while the shorter growth time would result in the higher R_{SH}. The optimal PCE of 3.8% could be achieved when the growth time is 35 min (Figure 3d), as an appropriate match consequence of the transmittance and sheet resistance.

In order to compare with the GNWs-MP solar cell, the graphene nanowall−planar Si (GNWs-Planar) solar cell was fabricated with the same growth time of 35 min. Figure 4a

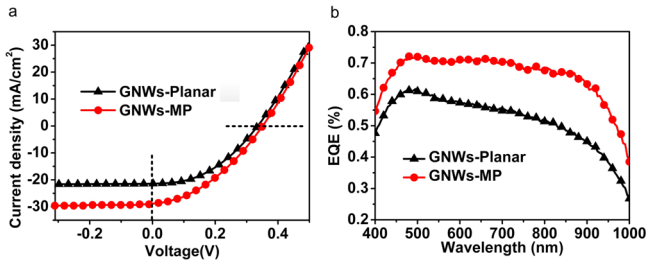

Figure 4. Comparison of (a) light J−V curves and (b) EQE of the GNWs-planar Si solar cell and GNWs-MP solar cell with same growth time of 35 min.

illustrates the photovoltaic performance. The J_{SC} of GNWs-Planar solar cell is only 21.2 mA/cm^2, while the J_{SC} of GNWs-MP solar cell could be enhanced to 28.7 mA/cm^2, implying the remarkable light absorption effect for the GNWs-MP solar cell. The external quantum efficiency (EQE) reflects the cells' capacity to capture incident photons into electricity.The EQE is defined as EQE = $I_{ph}(\lambda)\cdot hc/P_{in}(\lambda)e\lambda$, where $I_{ph}(\lambda)$ is the photocurrent; $P_{in}(\lambda)$ is the incident light power as a function of wavelength λ; h, c, and e is the Planck's constant, speed of light in vacuum, and elementary charge, respectively.[26] The GNWs-Planar Si solar cell shows a EQE of 50−60% in the range of 500−900 nm, while the EQE of the GNWs-MP solar cell is larger and almost reaches 70% in the same range shown in Figure 4b, indicating the more efficient utilization of incident light for the GNWs-MP solar cell.

Although the GNWs-MP solar cell has obtained a PCE of 3.8%, the poor sheet resistance would be an obstacle for higher efficiency. It has been proven that metal nanowires could effectively enhance the conductivity of graphene.[27,28] Therefore, the AgNWs were brushed onto the surface of GNWs for better conducting film, which was called the brush-painting process.[29,30] The SEM image of the AgNWs-GNWs-MP wafer is shown in Figure 5a. These AgNWs with the length of tens of micrometers are irregularly wrapped on the MP surface, and randomly form an efficient conducting network. The AgNW network could bridge the grain boundaries and adjacent graphene sheets to provide effective transport channels, bringing on the reduction of the R_{SH}. After brushing the AgNWs, the $R_{SH}$is significantly reduced from 1280 to 42 Ω/sq. Meanwhile, the transmittance at 550 nm drops from 81.5% to 77.8%, as shown in Figure 5b.

Figure 5c shows that the photovoltaic performance of the solar cell which is obviously improved after brushing the AgNWs.

DOI: 10.1021/acsami.5b05565
ACS Appl. Mater. Interfaces 2015, 7, 20179−20183

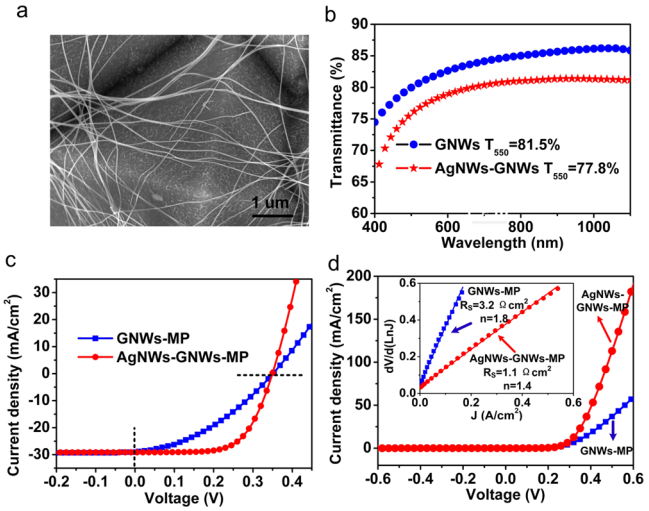

Figure 5. (a) SEM image of the morphology of GNWs-MP with wrapped AgNWs. (b) Transmittance of the GNWs and the AgNWs-GNWs film with growth time of 35 min. The comparison of the characteristics of GNWs-MP and AgNWs-GNWs-MP solar cells: (c) light $J-V$ curves; (d) dark $J-V$ curves. The inset of (d) shows the series resistance (R_S) and diode ideal factor (n) extracted from dark $J-V$ curves.

Compared with the intrinsic performance, the variations of the V_{OC} and J_{SC} are tiny, while the FF is remarkably enhanced from 38.0% to 64.4%, which corresponds to increasing rate of about 70%, and leads to a PCE of 6.6%. To better understand this phenomenon, the important parameters of series resistance (R_S) and diode ideal factor (n) are extracted from the dark $J-V$ curves for further analysis. The nonideal forward $J-V$ characteristics of the Schottky diode model can be expressed as[31]

$$J = J_S\left[\exp\left(\frac{q(V - IR_S)}{nkT}\right) - 1\right]$$

where q is the electronic charge, k is the Boltzmann constant, and J_S is the reverse saturation current density. The R_S is estimated from the slope of $d(V)/d(\ln J)$ versus J plot, and the n is calculated from the intercept.[32] From Figure 5d, it can be seen that the AgNWs-GNWs-MP solar cell has a larger forward current and the R_S could drop from 3.2 to 1.1 Ω cm^2 after AgNW brushing. This result clearly reflects more efficient transport for the AgNWs-GNWs-MP solar cell. Meanwhile, the n is 1.8 and 1.4 for the pristine and AgNWs-GNWs-MP solar cell, respectively. The reduction of n means the carrier recombination is inhibited, as a result of the reduction of R_S. Thus, the enhancement of the PCE is attributed to the AgNWs conducting network, which brings faster and more efficient carrier transport.

The stability of the solar cell is important to the practical application. In a previous report, $AuCl_3$ and volatile oxide, such as HNO_3 and $SOCl_2$, were used to chemically dope graphene or carbon nanotube (CNT).[33−35] However, the PCE of the doped solar cells gradually degraded after some time, because of the unstable chemical doping. We stored the AgNWs-GNWs-MP solar cell at 25 °C and 50% humidity without any encapsulation, and then detected the performance of the cell over time. The comparison with the reported chemically doped Gr-Si and CNT-Si solar cells is shown in Table 1. The photovoltaic performance of the AgNWs-GNWs-MP solar cell slightly degrades to 6.4%, only 3% loss after 20 days for the original efficiency (Supporting Information Figure S3). This stability is overwhelmingly superior

Table 1. Stability Comparison of the AgNWs-GNWs-MP Solar Cell with Previously Reported Chemically Doped Gr-Si and CNT-Si Solar Cells

type	original PCE	degraded PCE	degraded ration	storage time
Our work	6.6%	6.4%	3%	20 days
HNO_3-doped Gr-Si solar cell (ref 33)	5.47%	2.96%	46%	8 days
$SOCl_2$-doped Gr-Si solar cell (ref 33)	5.95%	3.29%	45%	8 days
$AuCl_3$-doped 4-layer graphene-Si solar cell (ref 34)	10.4%	9.65%	7.2%	7 days
HNO_3-dopedCNT-Si solar cell with encapsulation (ref 35)	10.9%	9.1%	17%	20 days

to that of the HNO_3-doped and $SOCl_2$-doped Gr-Si solar cells, and also exceeds the stabilities of the $AuCl_3$-doped few-layers graphene-Si solar cell and HNO_3-doped CNT-Si solar cell with encapsulation. For our solar cell, the decrease of the FF from 64.4% to 62.8% is the main cause for the PCE degradation, while the V_{OC} and J_{SC} mainly remain constant. The reason for the degradation may be that the AgNWs networks would be oxidized and eroded when exposed to the air for a long time.[36] The obvious surface roughness of AgNWs could be observed after 20 days exposure, as shown in Figure S4 (Supporting Information). This mechanism still needs additional related experiments to illuminate.

3. CONCLUSION

In summary, we reported a novel GNWs-MP solar cell produced by directly growing graphene nanowalls onto the micropyramidal Si substrate using a PECVD method. The optimal original efficiency of 3.8% occurs at the growth time of 35 min for the suitable combination of sheet resistance and transmittance. To further enhance the conductivity of the GNWs, we integrated AgNWs with GNWs by a simple brush-painting process, and achieved a low sheet resistance of 42 Ω/sq. A high efficiency of 6.6% is obtained from the AgNWs-GNWs-MP solar cell. Furthermore, this cell possesses good stability, compared with the reported chemically doped solar cells, only 3% degradation for the original PCE after storing in air for 20 days. These results present a simple way for low-cost, stable, high-efficiency, and environmentally friendly solar cells.

■ ASSOCIATED CONTENT

Supporting Information

The Supporting Information is available free of charge on the ACS Publications website at DOI: 10.1021/acsami.5b05565.

Table of characteristics of relevant solar cells studied in this work, SEM and reflectance of micropyramid Si with different etching time, $J-V$ curves of original and degraded AgNWs-GNWs-MP solar cells, SEM image of AgNWs after 20 days storage (PDF)

■ AUTHOR INFORMATION

Corresponding Authors

*E-mail: dpwei@cigit.ac.cn.

*E-mail: wtaosun@pku.edu.cn.

Author Contributions

#Tianpeng Jiao and Jian Liu contributed equally to this work and should be considered as co-first authors. The manuscript was

DOI: 10.1021/acsami.5b05565
ACS Appl. Mater. Interfaces 2015, 7, 20179−20183

written through contributions of all authors. All authors have given approval to the final version of the manuscript.

Notes

The authors declare no competing financial interest.

■ ACKNOWLEDGMENTS

This work was supported by NSFC (No. 11404329, No. 61306079), National High-tech R&D Program of China (863 Program, No. 2015AA034801), Natural Science Foundation Project of CQ CSTC (CSTC2014jcyjjq50004, cstc2012jjjq90001, cstc2012ggC50001, cstc2012ggC50003), and the Project-sponsored by SRF for ROCS, SEM.

■ REFERENCES

(1) Tyagi, V. V.; Rahim, N. A. A.; Rahim, N. A.; Selvaraj, J. A. L. Progress in Solar PV Technology: Research and Achievement. *Renewable Sustainable Energy Rev.* **2013**, *20*, 443−461.

(2) Parida, B.; Iniyan, S.; Goic, R. A Review of Solar Photovoltaic Technologies. *Renewable Sustainable Energy Rev.* **2011**, *15*, 1625−1636.

(3) Lewis, N. S. Toward Cost-Effective Solar Energy Use. *Science* **2007**, *315*, 798−801.

(4) Buonassisi, T.; Istratov, A. A.; Marcus, M. A.; Lai, B.; Cai, Z. H.; Heald, S. M.; Weber, E. R. Engineering Metal-Impurity Nanodefects for Low-Cost Solar Cells. *Nat. Mater.* **2005**, *4*, 676−679.

(5) Kim, K. S.; Zhao, Y.; Jang, H.; Lee, S. Y.; Kim, J. M.; Kim, K. S.; Ahn, J.-H.; Kim, P.; Choi, J.-Y.; Hong, B. H. Large-Scale Pattern Growth of Graphene Films for Stretchable Transparent Electrodes. *Nature* **2009**, *457*, 706−710.

(6) Geim, A. K.; Novoselov, K. S. The Rise of Graphene. *Nat. Mater.* **2007**, *6*, 183−191.

(7) Li, X. S.; Magnuson, C. W.; Venugopal, A.; An, J. H.; Suk, J. W.; Han, B. Y.; Borysiak, M.; Cai, W. W.; Velamakanni, A.; Zhu, Y. W.; Fu, L. F.; Vogel, E. M.; Voelkl, E.; Colombo, L.; Ruoff, R. S. Graphene Films with Large Domain Size by a Two-Step Chemical Vapor Deposition Process. *Nano Lett.* **2010**, *10*, 4328−4334.

(8) Li, X. M.; Zhu, H. W.; Wang, K. L.; Cao, A. Y.; Wei, J. Q.; Li, C. Y.; Jia, Y.; Li, Z.; Li, X.; Wu, D. H. Graphene-On-Silicon Schottky Junction Solar Cells. *Adv. Mater.* **2010**, *22*, 2743−2748.

(9) Lu, Y.; Lal, A. High-Efficiency Ordered Silicon Nano-Conical-Frustum Array Solar Cells by Self-Powered Parallel Electron Lithography. *Nano Lett.* **2010**, *10*, 4651−4656.

(10) Oh, J.; Yuan, H.-C.; Branz, H. M. An 18.2%-Efficient Black-Silicon Solar Cell Achieved through Control of Carrier Recombination in Nanostructures. *Nat. Nanotechnol.* **2012**, *7*, 743−748.

(11) Peng, K. Q.; Wang, X.; Li, L.; Wu, X. L.; Lee, S. T. High-Performance Silicon Nanohole Solar Cells. *J. Am. Chem. Soc.* **2010**, *132*, 6872−6873.

(12) Jeong, S.; Garnett, E. C.; Wang, S.; Yu, Z. G.; Fan, S. H.; Brongersma, M. L.; McGehee, M. D.; Cui, Y. Hybrid Silicon Nanocone-Polymer Solar Cells. *Nano Lett.* **2012**, *12*, 2971−2976.

(13) Xie, C.; Lv, P.; Nie, B.; Jie, J.; Zhang, X.; Wang, Z.; Jiang, P.; Hu, Z.; Luo, L.; Zhu, Z.; Wang, L.; Wu, C. Monolayer Graphene Film/Silicon Nanowire Array Schottky Junction Solar Cells. *Appl. Phys. Lett.* **2011**, *99*, 133113.

(14) Feng, T. T.; Xie, D.; Lin, Y. X.; Zhao, H. M.; Chen, Y.; Tian, H.; Ren, T. L.; Li, X.; Li, Z.; Wang, K. L.; Wu, D. H.; Zhu, H. W. Efficiency Enhancement of Graphene/Silicon-Pillar-Array Solar Cells by HNO_3 and PEDOT-PSS. *Nanoscale* **2012**, *4*, 2130−2133.

(15) Zhang, X.; Xie, C.; Jie, J.; Zhang, X.; Wu, Y.; Zhang, W. High-efficiency Graphene/Si Nanoarray Schottky Junction Solar Cells via Surface Modification and Graphene Doping. *J. Mater. Chem. A* **2013**, *1*, 6593−6601.

(16) Nistor, R. A.; Newns, D. M.; Martyna, G. J. The Role of Chemistry in Graphene Doping for Carbon-Based Electronics. *ACS Nano* **2011**, *5*, 3096−3103.

(17) Kong, X. K.; Chen, C. L.; Chen, Q. W. Doped Graphene for Metal-Free Catalysis. *Chem. Soc. Rev.* **2014**, *43*, 2841−2857.

(18) Shi, E.; Li, H.; Yang, L.; Zhang, L.; Li, Z.; Li, P.; Shang, Y.; Wu, S.; Li, X.; Wei, J.; Wang, K.; Zhu, H.; Wu, D.; Fang, Y.; Cao, A. Colloidal Antireflection Coating Improves Graphene-Silicon Solar Cells. *Nano Lett.* **2013**, *13*, 1776−1781.

(19) Yang, L.; Yu, X.; Xu, M.; Chen, H.; Yang, D. Interface Engineering for Efficient and Stable Chemical-Doping-Free Graphene-On-Silicon Solar Cells by Introducing a Graphene Oxide Interlayer. *J. Mater. Chem. A* **2014**, *2*, 16877−16883.

(20) Miao, X.; Tongay, S.; Petterson, M. K.; Berke, K.; Rinzler, A. G.; Appleton, B. R.; Hebard, A. F. High Efficiency Graphene Solar Cells by Chemical Doping. *Nano Lett.* **2012**, *12*, 2745−2750.

(21) Liang, X.; Sperling, B. A.; Calizo, I.; Cheng, G.; Hacker, C. A.; Zhang, Q.; Obeng, Y.; Yan, K.; Peng, H.; Li, Q.; Zhu, X.; Yuan, H.; Hight Walker, A. R.; Liu, Z.; Peng, L.-m.; Richter, C. A. Toward Clean and Crackless Transfer of Graphene. *ACS Nano* **2011**, *5*, 9144−9153.

(22) Li, X. S.; Zhu, Y. W.; Cai, W. W.; Borysiak, M.; Han, B. Y.; Chen, D.; Piner, R. D.; Colombo, L.; Ruoff, R. S. Transfer of Large-Area Graphene Films for High-Performance Transparent Conductive Electrodes. *Nano Lett.* **2009**, *9*, 4359−4363.

(23) Suk, J. W.; Kitt, A.; Magnuson, C. W.; Hao, Y.; Ahmed, S.; An, J.; Swan, A. K.; Goldberg, B. B.; Ruoff, R. S. Transfer of CVD-Grown Monolayer Graphene onto Arbitrary Substrates. *ACS Nano* **2011**, *5*, 6916−6924.

(24) Mao, S.; Yu, K.; Chang, J.; Steeber, D. A.; Ocola, L. E.; Chen, J. Direct Growth of Vertically-Oriented Graphene for Field-Effect Transistor Biosensor. *Sci. Rep.* **2013**, *3*, 1696.

(25) Yang, C.; Bi, H.; Wan, D.; Huang, F.; Xie, X.; Jiang, M. Direct PECVD Growth of Vertically Erected Graphene Walls on Dielectric Substrates as Excellent Multifunctional Electrodes. *J. Mater. Chem. A* **2013**, *1*, 770−775.

(26) Sayad, Y.; Amtablian, S.; Kaminski, A.; Blanc, D.; Carroy, P.; Nouiri, A.; Lemiti, M. Electrical Characterisation of Thin Silicon Layers by Light Beam Induced Current and Internal Quantum Efficiency Measurements. *Mater. Sci. Eng., B* **2009**, *165*, 67−70.

(27) Kholmanov, I. N.; Magnuson, C. W.; Aliev, A. E.; Li, H.; Zhang, B.; Suk, J. W.; Zhang, L. L.; Peng, E.; Mousavi, S. H.; Khanikaev, A. B.; Piner, R.; Shvets, G.; Ruoff, R. S. Improved Electrical Conductivity of Graphene Films Integrated with Metal Nanowires. *Nano Lett.* **2012**, *12*, 5679−5683.

(28) Choi, H. O.; Kim, D. W.; Kim, S. J.; Yang, S. B.; Jung, H. T. Role of 1D Metallic Nanowires in Polydomain Graphene for Highly Transparent Conducting Films. *Adv. Mater.* **2014**, *26*, 4575−4581.

(29) Kim, S. S.; Na, S. I.; Jo, J.; Tae, G.; Kim, D. Y. Efficient Polymer Solar Cells Fabricated by Simple Brush Painting. *Adv. Mater.* **2007**, *19*, 4410−4415.

(30) Lee, J.-H.; Shin, H.-S.; Noh, Y.-J.; Na, S.-I.; Kim, H.-K. Brush Painting of Transparent PEDOT/Ag Nanowire/PEDOT Multilayer Electrodes for Flexible Organic Solar Cells. *Sol. Energy Mater. Sol. Cells* **2013**, *114*, 15−23.

(31) Sze, S. M.; Ng, K. K. *Physics of Semiconductor Devices*; John Wiley & Sons: Hoboken, 2007.

(32) Cheung, S. K.; Cheung, N. W. Extractionof Schottky Diode Paramatersfrom Forward Current-Voltage Characteristics. *Appl. Phys. Lett.* **1986**, *49*, 85−87.

(33) Cui, T.; Lv, R.; Huang, Z.-H.; Chen, S.; Zhang, Z.; Gan, X.; Jia, Y.; Li, X.; Wang, K.; Wu, D.; Kang, F. Enhanced Efficiency of Graphene/Silicon Heterojunction Solar Cells by Molecular Doping. *J. Mater. Chem. A* **2013**, *1*, 5736−5740.

(34) Xie, C.; Zhang, X. J.; Ruan, K. Q.; Shao, Z. B.; Dhaliwal, S. S.; Wang, L.; Zhang, Q.; Zhang, X. W.; Jie, J. S. High-efficiency, Air Stable Graphene/SiMicro-Hole Array Schottky Junction Solar Cells. *J. Mater. Chem. A* **2013**, *1*, 15348−15354.

(35) Jia, Y.; Li, P.; Gui, X.; Wei, J.; Wang, K.; Zhu, H.; Wu, D.; Zhang, L.; Cao, A.; Xu, Y. Encapsulated Carbon Nanotube-Oxide-Silicon Solar Cells with Stable 10% Efficiency. *Appl. Phys. Lett.* **2011**, *98*, 133115.

(36) Mayousse, C.; Celle, C.; Fraczkiewicz, A.; Simonato, J. P. Stability of Silver Nanowire Based Electrodes under Environmental and Electrical Stresses. *Nanoscale* **2015**, *7*, 2107−2115.

DOI: 10.1021/acsami.5b05565
ACS Appl. Mater. Interfaces 2015, 7, 20179−20183